

## Relationship between superconductor and metal-insulator transitions in a large class of tetragonal 1:2:3 cuprates Ca-R-Ba-Cu-O ( $R=La,Nd$ )

D. Goldschmidt, A. Knizhnik, Y. Direktovitch, G.M. Reisner, and Y. Eckstein  
*Department of Physics and Crown Center for Superconductivity, Technion, Haifa 32000, Israel*  
 (Received 27 February 1995; revised manuscript received 16 May 1995)

We report superconductor and transport properties of a large class of tetragonal 1:2:3 cuprates represented by the chemical formula  $(Ca_xR_{1-x})[Ba_{3-z-x}R_{z-(1-x)}]Cu_3O_y$ , where  $R=La$  or  $Nd$  and existing as high-purity materials in a large range of  $z$  and  $x$ . At a given  $z$ , these materials maintain, through compensating cosubstitutions, a constant charge  $Q$  of the noncopper cations ( $Q=6+z$ ) independent of  $x$ . By accurate control of oxygen content  $y$ , both cation and anion charge sources were kept constant. Under these isoelectronic conditions (constant electron concentration  $n$ ) big changes in transition temperature  $T_c$ , resistivity  $\rho$  and thermopower (TEP)  $S$  occur, suggesting that the microscopic hole density in the  $CuO_2$  planes  $h$  changes. Having a single  $T_c^{max}$  (maximal  $T_c$ ), this material family behaves as a single material. Besides, for all values of  $Q$ ,  $x$ , and  $y$  and for each  $R$  we show that  $T_c$ ,  $\rho$ , and  $S$  can each be represented by a single curve when plotted as a function of  $y-y_{M-I}(Q,x)$ , where  $y_{M-I}$  denotes the value of  $y$  at the metal-insulator (M-I) transition. Therefore, there exists a one to one correspondence between  $h$  and  $y-y_{M-I}$ , but there is no straightforward relation between  $h$  and  $n$ . We found an empirical formula describing the functional dependence of  $y_{M-I}$  on  $Q$  and  $x$ . This allows one to estimate  $y_{M-I}$ ,  $T_c$ ,  $\rho$ , and  $S$  in many materials. Our results are interpreted in terms of a simple band picture which is modified to consider the existence of low-mobility states in the vicinity of  $E_F$ . This accounts for the relatively low TEP at the M-I transition.

### I. INTRODUCTION

In spite of much experimental work, the relation in cuprate superconductors between transition temperature or transport properties and hole density remains an unresolved problem. Not only do we lack a sound theoretical basis for the understanding of such relations but also there seems to be no consensus as to how the microscopic hole density in the  $CuO_2$  planes should be estimated.<sup>1</sup> Methods borrowed from semiconductors that are intended to measure the microscopic hole density such as Hall effect and thermoelectric power, or structural methods such as bond valence sums, have not yet reached a consensus. Another method of estimating the microscopic hole density relies on determination of some average macroscopic hole concentration such as based on the chemical charge that is derived from valence. For instance, it is well known in  $La_{2-x}Sr_xCuO_4$  that the transition temperature  $T_c$  increases upon substitution of Sr until at  $x=0.15$  it reaches a maximum and then it gradually disappears at higher values of  $x$ . It is believed, even though not established beyond any doubt, that each substituted Sr atom adds one hole to the  $CuO_2$ -plane band.

It has recently been shown that similar doping effects exist in  $YBa_2Cu_3O_{6.96}$ , where the oxygen content was kept constant.<sup>2</sup> Here  $T_c$  was changed either by substitution of  $Ca^{2+}$  for  $Y^{3+}$  or of  $La^{3+}$  for  $Ba^{2+}$ . The effect on  $T_c$  of these substitutions bears a striking symmetry. The dependence of  $T_c$  on the concentration of the substituted atoms falls on the same curve (i.e., a smooth parabola) irrespective of whether one substitutes Ca or La (see Fig. 1 in Ref. 2). This would mean that a given amount of either substitution has the same effect on  $T_c$  (but, of course, of opposite sign) and hence also

on the microscopic hole density. This seems to suggest that when Ca and La are cosubstituted in equal amounts, one substitution will fully counteract the effect of the other and full compensation would be expected. In other words, the microscopic hole density remains constant and no doping effects should be observed. It was further suggested that substitution of one Ca or La atom introduces one hole or one electron in the planes, respectively.<sup>2</sup> This implies that, under conditions where the oxygen content remains constant, a simple one to one relationship between the microscopic hole density and the chemical hole concentration might exist. (We would like to emphasize that we distinguish here between the chemical hole concentration, which is a macroscopic average determined from valence, and the microscopic density of mobile holes in the  $CuO_2$  planes. We also caution in advance that in many cases a one to one relationship between both quantities does not hold, as will be explained in the Discussion.)

It is well known that the hole density can be varied also by changing the oxygen content. This, however, complicates the hole counting considerably, because the contribution of each charge source (i.e., cation or oxygen) to the actual hole density is not known. Tokura *et al.*<sup>3</sup> suggested an empirical formula for estimating  $h$  the microscopic hole density per  $CuO_2$  layer. We have shown<sup>4</sup> that this formula can also be written as  $h=\frac{1}{2}(y-Q+\frac{1}{2})$ , where  $y$  denotes the oxygen (or anion) content and  $Q$  is the total chemical charge of the noncopper cations as determined from summation of their valence. The approach of Tokura *et al.* suggests that  $h$  is completely determined by  $y$  and  $Q$ . However, we have shown recently that this relationship does not always yield the correct estimate of mobile hole density.<sup>5,6</sup> The problem of unknown contributions to  $h$  when both anion and cation charges change simultaneously, can be avoided in compen-

sated materials, where the cation charge source is held constant while some chemical parameter is varied. If the anion charge source can also be controlled, this would allow investigation of physical properties under more controlled conditions.

Recently, we have investigated the tetragonal 1:2:3 family of materials  $(\text{Ca}_x\text{La}_{1-x})(\text{Ba}_{1.75-x}\text{La}_{0.25+x})\text{Cu}_3\text{O}_y$  (CaLaBaCuO).<sup>6,7</sup> This family is charge compensated through equal amounts of  $\text{Ca}^{2+}$  and  $\text{La}^{3+}$  cosubstitutions on the  $\text{Y}^{3+}$  site (first bracket) and  $\text{Ba}^{2+}$  site (second bracket) of the 1:2:3 structure, respectively. Hence, in this family,  $Q$  is constant independent of  $x$ ,  $Q = 2x + 3(1-x) + 2(1.75-x) + 3(0.25+x) = 7.25$ , provided that each noncopper cation preserves its regular valence in these materials (+2, +2 and +3 for Ca, Ba, and La, respectively). By fine control and accurate measurement of oxygen content  $y$ ,<sup>6,8</sup> we have shown that a single macroscopic parameter  $y - y_{\text{M-I}}(x)$  controls the behavior of many physical properties for all values of  $x$  and  $y$ .<sup>9</sup> These properties include the superconductor transition temperature  $T_c$ , the resistivity  $\rho$ , and the room-temperature thermoelectric power (TEP)  $S$ . Hence, we postulate that  $y - y_{\text{M-I}}(x)$  is the appropriate macroscopic doping parameter in these materials, that is,  $h$  is a function of  $y - y_{\text{M-I}}(x)$ . This parameter denotes the departure in oxygen content  $y$  from its value at the metal-insulator (M-I) transition  $y_{\text{M-I}}$ . It allows for a change in hole density  $h$  also under isoelectronic conditions, that is, when the macroscopic hole concentration remains constant. Such conditions are materialized by keeping  $y$  constant because  $Q$  is anyway constant when  $x$  changes. In that case  $h$  could still change since  $y_{\text{M-I}}$  varies with  $x$ . Our very recent pressure ( $P$ ) measurements also suggest that there is a one to one correspondence between  $h$  and  $y - y_{\text{M-I}}(x)$ .<sup>10</sup> It is well known that the pressure derivative  $dT_c/dP$  is strongly dependent on the doping level  $h$  decreasing in going from underdoped to overdoped materials.<sup>11</sup> We have shown that in CaLaBaCuO the dependence of  $dT_c/dP$  on  $h$  can be replaced by a simple dependence on  $y - y_{\text{M-I}}(x)$ .<sup>10</sup>

Another interesting property of the CaLaBaCuO family is its tetragonal structure<sup>7</sup> throughout the range of existence which, as we show in this work, comprises  $0 \leq x \leq \sim 0.5$  and  $\sim 6.4 \leq y \leq 7.15$ . This higher symmetry of CaLaBaCuO as compared to the more investigated orthorhombic 1:2:3 cuprates is important as it avoids complications due to long-range chain order and to structural phase transitions which would obscure the simple behavior that we observed. In short, this family is simpler than the frequently investigated YBaCuO family.

In this paper we extend our study to other 1:2:3 charge compensated families, each with a different value of  $Q$ , and to other trivalent rare earth ( $R$ ) constituents. These materials can be represented by the chemical formula  $(\text{Ca}_x\text{R}_{1-x})(\text{Ba}_{3-z-x}\text{R}_{z-(1-x)})\text{Cu}_3\text{O}_y$ ; whence,  $Q = 2x + 3(1-x) + 2(3-z-x) + 3[z-(1-x)] = 6+z$ . The material family that we investigated in previous work<sup>6,7</sup> and was described above corresponds to  $z = 1.25$  ( $Q = 7.25$ ). In the present study we prepared new materials having  $R = \text{La}$  or  $\text{Nd}$  and different values of  $Q$  which were obtained through variation of the ratio between  $R$  and Ba (Sec. II). For  $R = \text{La}$ , we show in this work (Sec. III A) that materials exist in single phase in the range  $\sim 7 \leq Q \leq 7.5$  ( $1 \leq z \leq 1.5$ ) and  $\sim 0 \leq x \leq \sim 0.5$ .

(This is consistent with other recent investigations.<sup>12</sup>) We show that there exists a single  $T_c^{\text{max}}$  for all materials, where  $T_c^{\text{max}}$  denotes the maximal value of  $T_c$  attainable by doping. Thus all compositions (various values of  $Q$  and  $x$  as well as both rare earth substitutions  $R$ ) behave like a single family of materials in the sense that many physical properties vary smoothly and in a predictable manner from one composition to another. Moreover, we also show that the same single doping parameter  $y - y_{\text{M-I}}(Q, x, R)$  determines the properties of this extended family and that  $y_{\text{M-I}}$  now varies both as function of  $Q$  and of  $x$  but is nearly independent of  $R$  for the two species investigated. We developed an accurate method for determining the experimental value of  $y_{\text{M-I}}$  (Sec. III B). Based on measurements on a number of compositions of CaLaBaCuO materials, we also find an empirical formula that allows one to extrapolate new values of  $y_{\text{M-I}}(Q, x)$  (Sec. III B 3). These empirical values compare well with the measured values. This extrapolation is valid as long as the materials remain tetragonal. We use this procedure to obtain  $y - y_{\text{M-I}}(Q, x)$  in the entire family from which one could estimate physical properties such as  $T_c$ ,  $\rho$ , and  $S$ . In this way it becomes possible to make such estimates without actually preparing the materials. In particular, it circumvents the laborious determination of  $y_{\text{M-I}}$  in many materials. Finally, in Sec. IV we discuss the implications of our results on current doping theories within the band and correlation pictures.

## II. EXPERIMENT

Our samples were prepared by reaction of solid oxide and carbonate powders. The starting materials were  $\text{La}_2\text{O}_3$  (99.98% pure),  $\text{Nd}_2\text{O}_3$  (>99.9%),  $\text{CuO}$  (>99%),  $\text{BaCO}_3$  (>99%), and  $\text{CaCO}_3$  (>99%). In order to remove water or hydroxides, the oxides  $\text{La}_2\text{O}_3$ ,  $\text{Nd}_2\text{O}_3$  and the carbonates  $\text{BaCO}_3$ ,  $\text{CaCO}_3$  have been preheated in  $\text{O}_2$  for 48 h at 1100 °C and 450 °C, respectively, cooled in a dessicator and weighted in stoichiometric proportions in a glove bag containing dry Ar. The raw materials were mixed in a powder mixer and ground for half an hour in a zirconia ball mill. The powder was fired for 16–20 h in a box furnace in air, transferred from the hot furnace into a dry dessicator, and re-ground with an Agate mortar and pestle. The firing temperature was 930 °C–950 °C for  $R = \text{La}$ ,  $\text{Nd}$  and  $Q = 7.25$ , increasing to 950 °C–980 °C for  $R = \text{La}$  and  $Q = 7.35, 7.45$ . These firings were repeated 3–4 times until small shiny crystallites appeared and no impurity phases were observed. The fine powders were pelletized into a bar shape measuring  $2.5 \times 2.5 \times 13 \text{ mm}^3$  and containing a linear array of four implanted gold wires under a pressure of 5 kbar applied to the surface containing the wires. The  $Q = 7.25$  ( $R = \text{La}, \text{Nd}$ ) pellets were sintered for 60–70 h at temperatures of 950 °C–960 °C in a tube furnace containing slowly flowing dry  $\text{O}_2$ . For the samples containing more La ( $Q = 7.35, 7.45$ ) we raised the sintering temperature to 980 °C at which a period of 10 h was sufficient to yield good samples. The cooling of samples in the tube furnace included soaks at 600, 500, 450, 400, 350, 320, 300, and 280 °C of duration 5 or 25 h each at the higher or lower soak temperatures, respectively. After furnace cool down the samples were removed at room temperature. These “as-prepared” samples have the highest oxygen content reported in this work, e.g.,  $y = 7.15$  or 7.23 for

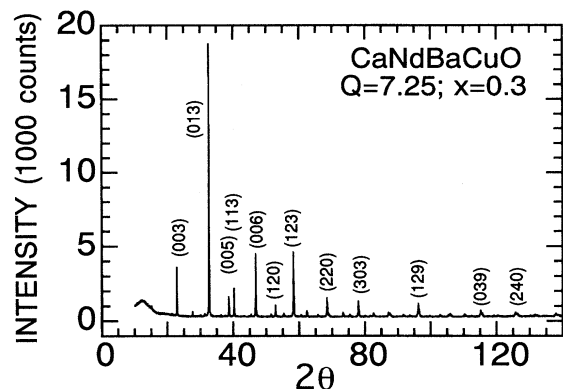


FIG. 1. Typical x-ray-diffraction spectrum of  $(\text{Ca}_x\text{Nd}_{1-x})(\text{Ba}_{1.75-x}\text{Nd}_{0.25+x})\text{Cu}_3\text{O}_y$ . All lines were indexed according to the tetragonal  $P4/mmm$  space group (only indices of the strong lines are shown).

$Q=7.25$  or  $7.45$ , respectively (in both cases  $R=\text{La}$  and  $x=0.4$ ). Reduction of the samples was done in a vertical tube furnace containing slowly flowing dry  $\text{O}_2$  or  $\text{Ar}$  gas. After holding a sample for over 16 h in the furnace it was quenched by quick immersion in liquid  $\text{N}_2$ . The annealing temperature for a specific reduction depends on the value of  $x$ ,  $Q$ , and  $y$  and on the gas used. For  $y \geq 6.6$  samples were annealed in  $\text{O}_2$  in the temperature range between 350 and 950 °C corresponding roughly to a decrease in  $y$  by 0.1 for each 100 °C increase in annealing temperature. For lower  $y$  ( $6.4 \leq y \leq 6.6$ ), annealing in  $\text{Ar}$  (or  $\text{N}_2$ ) gas at temperatures up to 910 °C was employed. Where possible, annealing in  $\text{O}_2$  should be preferred as the higher annealing temperature at a given  $y$  yields better homogeneity of oxygen distribution.

The lowest oxygen content before decomposition occurs is  $y \approx 6.4$  in  $\text{CaLaBaCuO}$  with  $Q=7.25$ . For instance, the  $x=0.1$  composition is pure for  $y=6.42$  while showing impurities for slightly lower oxygen content. For  $y \geq 6.4$ , our samples are of high phase purity. This can be seen in Fig. 1 where we plotted the x-ray-diffraction (XRD) spectrum of  $\text{CaNdBaCuO}$  ( $Q=7.25, x=0.3$ ). Further details are given in Refs. 6 and 7. The upper stability limit of the  $Q=7.25$   $\text{CaLaBaCuO}$  is  $x \approx 0.5$ . In fact, the  $x=0.5$  material is not easily obtained with the high purity typical of the other compositions implying that the stability limit could actually be slightly less than 0.5. There is though no problem with preparing the pure  $x=0.45$  material. On the other side of the stability range, at  $x=0$ , pure phase can also be prepared. However, the physical properties (e.g., transition width) of the reduced  $x=0$  samples are not as good as in other compositions. Therefore we do not report investigation of the  $x=0$  samples. In  $\text{CaNdBaCuO}$  we did not succeed in producing a high-purity phase of composition  $x=0.4$ . Thus the  $x=0.3$  composition may be considered as the approximate upper stability limit for  $R=\text{Nd}$ ,  $Q=7.25$ .

Homogeneity of oxygen distribution within a grain and among grains was verified indirectly by the small width of the resistive and susceptibility transitions, respectively.<sup>6,7</sup>

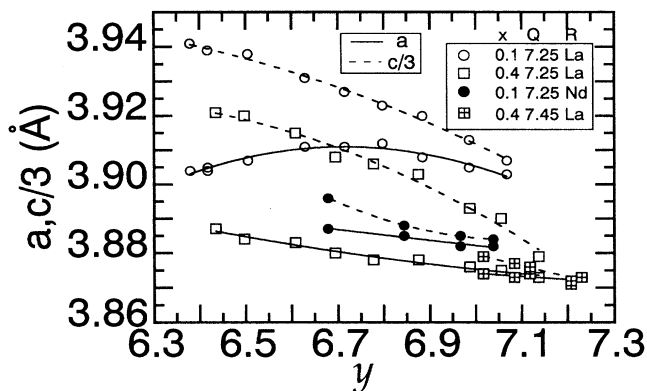


FIG. 2. Lattice parameters vs oxygen content  $y$  for various compositions  $x$ .

Generally speaking, the resistive transition width increases with decreasing oxygen content from  $\sim 1$  K in the vicinity of optimal doping to  $\sim 6$  K near the M-I transition. On the other hand, the degree of cation disorder, which is changing with  $x$ , does not seem to have any significant effect on the transition width. Oxygen content was determined by iodometric titration using a microburette and other precautions.<sup>6,8</sup> We performed three titrations, each on a mass of 5 mg that was extracted from a sample and crushed into powder. One of these titrations was used to measure the total copper content within the sample and, per one 1:2:3 formula unit, corresponded to  $3.000 \pm 0.005$ . (This titration was calibrated against a carefully-prepared  $\text{CuO}$  solution.<sup>8</sup>) This is an upper limit on the error in the copper content. The reproducibility among various samples was better ( $\pm 0.003$ ). This titration together with the other two titrations then yielded the oxygen content assuming that the valence of oxygen is  $-2$ . The reproducibility between the two titrations made on the same sample was about  $\Delta y = \pm 0.002$ . The random error between samples would not exceed much this value as is indicated by the minimal scatter in our data. This seems to suggest that our samples contain practically no impurity phases or at least that the amount of impurities is sample independent.

We measured the resistivity ( $I=10$  mA),<sup>7</sup> dynamic thermoelectric power  $dV/dT$  ( $\Delta T \leq 0.5$  K),<sup>9</sup> and ac magnetic susceptibility<sup>7</sup> ( $H=25$  mOe) of our samples using standard procedures. The values in parentheses denote, respectively, the current, maximal temperature difference and magnetic field used in these measurements. Our routine was to measure resistivity and TEP on the entire sample, then split it and measure ac susceptibility, oxygen content, and XRD.

### III. RESULTS

#### A. Lattice parameters

In Fig. 2 we present the tetragonal lattice parameters  $a$  and  $c$  of various samples as function of oxygen content  $y$ . There is a general trend of increase in lattice parameters as the oxygen content decreases, which is common to many cuprates. This trend is reversed in the  $a$  lattice parameter of the  $Q=7.25, x=0.1$   $\text{CaLaBaCuO}$ . This opposing trend oc-

curs for no apparent reason; it begins at  $y \cong 6.8$ , that is, much below the M-I transition that occurs at  $y \cong 7$  (see below). Interestingly, the lattice parameters of the  $Q=7.45$ ,  $x=0.4$  CaLaBaCuO are almost constant as a function of  $y$  in a range that includes materials well within the insulating phase together with materials well within the superconducting phase having  $T_c$  as high as 65 K. A similar behavior was observed in the  $Q=7.25$ ,  $x=0.1$  CaNdBaCuO where the lattice parameters vary only slightly. It seems that the magnitude of the lattice parameter has no direct effect on  $T_c$ . This becomes more evident when comparing samples having the same  $T_c$  [that is, with the same value of  $y - y_{M-I}(Q, x)$ ] but with different lattice parameters. Compare, for instance, in Fig. 2 the  $R=La$  sample with  $Q=7.25$ ,  $x=0.1$ ,  $y=7.068$  to that with  $Q=7.25$ ,  $x=0.4$ ,  $y=6.987$ . For both samples we observed  $T_c = 46$  K and  $y - y_{M-I} \cong 0.09$ , but the lattice parameters vary significantly ( $a$  decreases from 3.903 to 3.876 Å and  $c/3$  from 3.907 Å to 3.893 Å). This change in lattice parameters between both samples ( $\Delta a/a = 0.7\%$ ,  $\Delta c/c = 0.35\%$ ) represents a large fraction of the change which occurs in each composition over its entire range of superconductivity.

## B. The metal-insulator transition

### 1. Dependence of $T_c$ on oxygen content

We would like to establish an accurate method to determine  $y_{M-I}$ . The M-I transition was identified with full suppression of superconductivity, i.e., when  $T_c \rightarrow 0$  K. In principle,  $y_{M-I}$  could be estimated by observation of the dependence of  $T_c$  on  $y$ , as shown in Fig. 3 for  $Q=7.25$  and  $x=0.4$ . However, even though this composition represents our most detailed and accurate set of data, it is still hard to extrapolate near the M-I transition due to the sharp dependence of  $T_c$  on  $y$ . Therefore we employed a different procedure that makes use of our most reliable data further away from the M-I boundary and also assumes that the dependence of  $T_c$  on  $y$  provides only a lower limit of  $y_{M-I}$  since superconductivity disappears for all samples in which  $y \leq y_{M-I}$ . Consider first the following compositions: CaLaBaCuO (i.e.,  $R=La$ ) with  $Q=7.25$  and  $x=0.1, 0.2, 0.3, 0.4$  as well as with  $x=0.4$  and  $Q=7.35, 7.45$ . We use this subset of materials to investigate the behavior of  $y_{M-I}$  and then use the result to extrapolate new values of  $y_{M-I}$  in other materials. The results of  $T_c$  vs  $y$  for these materials are shown in Fig. 3 (for the meaning of  $T_{c,ext}^R$ , see the inset of Fig. 4). Clearly,  $y_{M-I}$  varies with both  $Q$  and  $x$ . At a given  $x$ , the curves for various values of  $Q$  are well separated from one another [Fig. 3(a)]. Interestingly, all curves are almost parallel to one another. This means that for a given  $(Q, x)$  one can find a quantity  $\Delta y(Q, x)$  such that when these  $T_c$  results are plotted against  $y - \Delta y(Q, x)$ , all curves in Fig. 3 coalesce into a single curve. This is demonstrated in Fig. 4 for  $x=0.4$  and  $Q=7.25$  and  $7.35$ . The values of  $y$  on the abscissa are those corresponding to  $Q=7.25$ ,  $x=0.4$ . In other words,  $\Delta y(7.25, 0.4) = 0$ , making this curve identical with the corresponding curve in Fig. 3. For the curve  $Q=7.35$ ,  $x=0.4$  we plotted in Fig. 4 also  $T_c$  as function of  $y - \Delta y(7.35, 0.4)$ , where we use for  $T_{c,ext}^R$ ,  $\Delta y(7.35, 0.4) = 0.093$ . This value of  $\Delta y$  was chosen so that both curves coincide not near  $y_{M-I}$ ,

where the data points are somewhat scattered, but rather in the range  $6.92 \leq y \leq 7.12$ , where for samples having the same  $T_c$  the scatter in  $y$  is less than 0.001. This range contains most of our data and the determination of  $\Delta y$  becomes quite accurate. The same procedure has been applied to the other curves in Fig. 3 (not shown). Notice that the shift  $\Delta y(Q, x)$  obtained in this way is uniform independent of  $y$ , that is, it is one and the same for all samples with a given  $Q$  and  $x$ . It is noted that the coalescence into a single curve requires that the  $T_c$  vs  $y$  data points essentially have no scatter, as is the case in Fig. 3 and in most of our other data.

### 2. Experimental determination of the oxygen content $y_{M-I}$ at the metal-insulator transition

We proceed with the determination of  $y_{M-I}(Q, x)$  where the first step was the plot of  $T_c$  vs  $y - \Delta y(Q, x)$  as in Fig. 4. We assume that  $y_{M-I}$  is obtained from the highest value of  $y - \Delta y$  for which  $T_c$  still remains zero. Placing together all  $T_c(y)$  curves of the preselected subset of materials (Sec. III B 1), this highest value is determined quite accurately, as it relies on many data points in the oxygen range ( $6.92 \leq y - \Delta y \leq 7.12$ ) where the scatter in our data is minimal as well as on many other points below the M-I transition for which  $T_c = 0$  K. In this way, the accuracy in the determination of  $y_{M-I}$  does not suffer from the relatively large scatter in  $T_c$  near the M-I boundary itself. In Fig. 4, the highest value of  $y$  at which  $T_c$  is still 0 K occurs at 6.907. This value then represents  $y_{M-I}(7.25, 0.4)$  as obtained from  $T_{c,ext}^R$ . For any other curve with a specific value of  $Q$  and  $x$  such as  $Q=7.35, x=0.4$  in Fig. 4, we find  $y_{M-I}(Q, x)$  by adding to the value of  $y_{M-I}(7.25, 0.4)$  the value of  $\Delta y(Q, x)$  found earlier (as in producing Fig. 4). These constitute the experimental values of  $y_{M-I}(Q, x)$  in Table I, as determined from  $T_{c,ext}^R$ . The error in estimating the point where  $T_c \rightarrow 0$  K according to this procedure is about  $\pm 0.002$ , as determined from the scatter of data points having  $T_c = 0$  K (see Figs. 4 and 5). The additional random error in the determination of  $y$  is estimated also to be  $\pm 0.002$  (Sec. II). Thus the total random error in determining  $y_{M-I}(Q, x)$  is about  $\pm 0.003$ .

It is possible to use the same procedure but other definitions of  $T_c$  in order to obtain  $y_{M-I}$ . For instance, one could use  $T_{c,onset}^R$ , the resistive onset of the superconductor transition which represents properties of the intragranular phase.<sup>6</sup> As the transition broadens with lowering of the oxygen content, it might be interesting to examine the effect of other definitions of  $T_c$  on the value of  $y_{M-I}$ . We examined the following definitions as shown in the inset of Fig. 4:  $T_{c,onset}^R$ ,  $T_{c,0}^R$ ,  $T_c^X$ , and  $T_{c,ext}^R$ , which, respectively, denote the resistive onset, the zero resistance (i.e., end of tail), the onset of the strong ac susceptibility (i.e., that related with the connectivity of the grain boundaries<sup>6</sup>), and the extrapolated transition temperature, corresponding to the disappearance of the intragranular resistivity (i.e., the temperature where the resistivity would drop to zero had there been no tail due to grain boundaries or other effects).  $T_{c,ext}^R$  was obtained by extrapolating the steep edge of the resistive transition to zero resistance. Each definition of  $T_c$  yields a slightly different value of  $y_{M-I}$ . It turns out that the measured average value  $y_{M-I}^{av}$ , displayed on the right side of Table I, is best represented by the values obtained from  $T_{c,ext}^R$ , i.e., when some fraction of

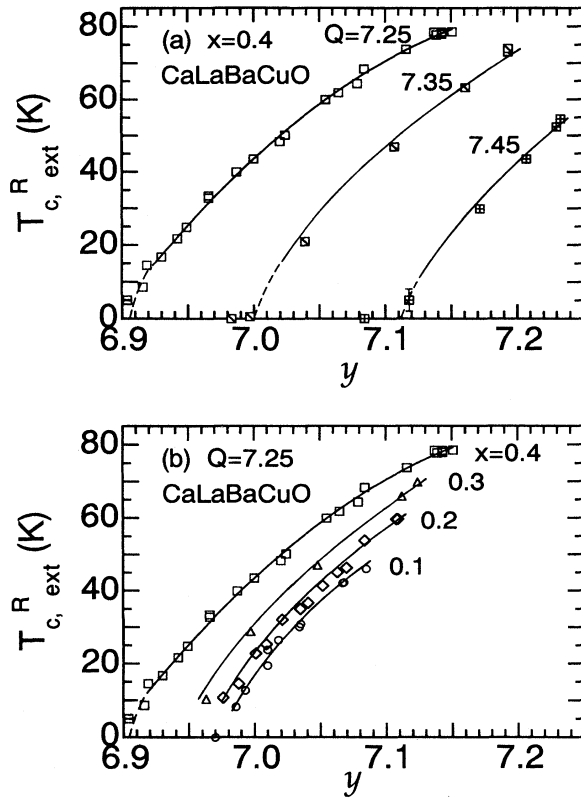


FIG. 3. The dependence of the resistive  $T_c$  on oxygen content  $y$  (a) at various values of the cation charge  $Q$ , and (b) at various compositions  $x$ . Notice that the curves are almost parallel one to the other.

the intragranular material has become superconductor. The error in  $y_{M-I}^{av}$ , does not exceed  $\pm 0.005$  in most cases.

So far we have used a subset of our samples including only a number of compositions. These are marked in bold-face in Table I. We now return to the entire set of our samples including the previous subset (Sec. III B 1) as well as the other  $R=La$ ,  $Q=7.45$ ,  $x=0.2$ , and  $R=Nd$ ,  $Q=7.25$ , and  $x=0.1, 0.2, 0.3$  compositions. The results of  $T_c$  vs  $y - y_{M-I}$  as obtained by the various definitions are plotted in Fig. 5. Notice the coalescence into a single curve of all our data points with only limited scatter. This is a result of the high accuracy in our data as can be obtained in this class of materials. [The larger scatter close to the M-I boundary is a result of the sharpening of the dependence of  $T_c$  on  $y$  in that range, particularly evident in Fig. 5(a). As was explained above, this scatter does not affect the accuracy in the determination of  $y_{M-I}$ .] The coalescence into a single curve is also an indication that all materials investigated in this study have the same  $T_c^{max}$ . For instance, in Fig. 5(a),  $T_{c,onset}^{R,max} = 82$  K. (Even though this value is not actually attained in this figure as our most oxidized sample is still slightly on the underdoped side,  $T_{c,onset}^{R,max}$  can be obtained from a parabolic fit of our  $T_{c,onset}^R$  vs  $y - y_{M-I}$  data.<sup>10</sup>) In Sec. IV we provide more evidence for the existence of a single  $T_c^{max}$ . This strongly suggests that the extended class of materials (including La

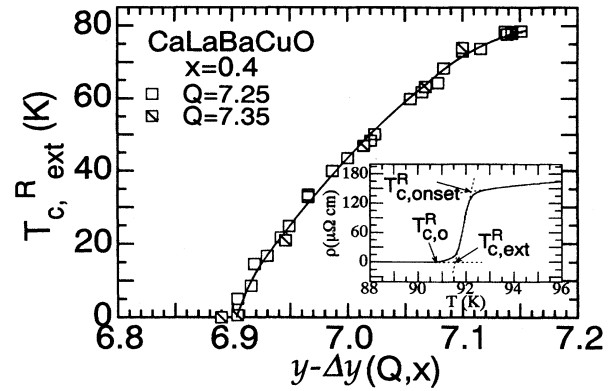


FIG. 4. The dependence of  $T_c$  on oxygen content in two materials. The abscissa denotes a shifted scale of oxygen content. The curves have been shifted so that they coincide in the range  $6.92 \leq y \leq 7.12$  (see text). Inset: various definitions of  $T_c$ .

and Nd and all values of  $Q$  and  $x$ ) behaves as a single material family (actually as a single material) at least as long as the materials remain tetragonal.

### 3. Empirical formula of $y_{M-I}$ as function of $Q$ and $x$

We now turn to the investigation of the functional dependence of  $y_{M-I}$  on  $Q$  and  $x$ . (In principle,  $y_{M-I}$  could also be a function of  $R$ , the type of rare earth ion. However, examination of Table I shows that no systematic change occurs upon going from  $R=La$  to  $R=Nd$ .) Besides fundamental interest in finding trends in the behavior of the M-I transition this investigation is important, allowing one to predict values of  $y_{M-I}$  for families of materials that have not actually been prepared. Therefore, we use for this purpose again only the subset selected in Sec. III B 1 and then extrapolate to the rest of the materials. We begin by holding  $x$  constant ( $x=0.4$ ) and varying  $Q$  [Fig. 6(a)], using the measured average values  $y_{M-I}^{av}$  (see Table I). The dependence of  $y_{M-I}^{av}$  on  $Q$  is linear. We then plot in Fig. 6(b)  $y_{M-I}^{av}$  as function of  $x$  at constant  $Q (=7.25)$ . The dependence that we obtained in this case by fitting to our results is nearly quadratic. These results can be casted into a simple empirical formula:

$$y_{M-I}^{av}(Q,x) = y_{M-I}^{av}(Q_0,x_0) + \alpha(Q - Q_0) - \beta(x - x_0)^2. \quad (1)$$

The parameters that we obtained by fitting to the results of  $y_{M-I}^{av}$  in Fig. 6 are approximately  $y_{M-I}(Q_0,x_0) = 6.98$ ,  $\alpha \cong 1$ ,  $\beta \cong 0.5$ ,  $Q_0 = 7.25$ , and  $x_0 \cong 0$ . The value of  $Q_0$  that we chose is arbitrary. More accurate values for  $\alpha$  and  $\beta$  are  $0.99 \pm 0.06$  and  $0.438 \pm 0.027$ , respectively, as estimated from the error bars.

We used the more accurate values of these parameters to estimate  $y_{M-I}(Q,x)$  for the entire set of compositions including the previous subset. These calculated values of  $y_{M-I}^{av}$  are also shown in Table I. The agreement between the calculated and measured values of  $y_{M-I}$  is very good. (See Fig. 7.) In particular, for those samples that were not used in obtaining

TABLE I. The value of  $y_{M-I}$ , the oxygen content at the metal-insulator transition, obtained according to various definitions of  $T_c$  (see inset, Fig. 4). The average measured values should be compared to the calculated values obtained from Eq. (1). (Values in parentheses represent standard deviation of the last decimal figure.) Values in boldface are those that were used in deriving the parameters of Eq. (1), namely,  $y_{M-I}^{av}(Q,x) = 6.98 + 0.99(Q - 7.25) - 0.438x^2$ .

Substance	$Q$	$x$	$y_{M-I}$ as obtained from				$y_{M-I}^{av}$ measured	$y_{M-I}^{av}$ calc.
			$T_{c,onset}^R$	$T_{c,ext}^R$	$T_{c,0}^R$	$T_c^X$		
CaLaBaCuO	<b>7.25</b>	<b>0.1</b>	<b>6.972</b>	<b>6.977</b>	<b>6.980</b>	<b>6.975</b>	<b>6.976(3)</b>	<b>6.975(0)</b>
	<b>7.25</b>	<b>0.2</b>	<b>6.961</b>	<b>6.965</b>	<b>6.970</b>	<b>6.970</b>	<b>6.966(4)</b>	<b>6.963(1)</b>
	<b>7.25</b>	<b>0.3</b>	<b>6.938</b>	<b>6.945</b>	<b>6.945</b>	<b>6.948</b>	<b>6.944(4)</b>	<b>6.941(2)</b>
	<b>7.25</b>	<b>0.4</b>	<b>6.900</b>	<b>6.907</b>	<b>6.910</b>	<b>6.912</b>	<b>6.907(5)</b>	<b>6.910(4)</b>
CaLaBaCuO	<b>7.35</b>	<b>0.4</b>	<b>6.985</b>	<b>7.000</b>	<b>7.000</b>		<b>6.995(7)</b>	<b>7.009(7)</b>
	<b>7.45</b>	<b>0.4</b>	<b>7.088</b>	<b>7.113</b>	<b>7.113</b>		<b>7.105(12)</b>	<b>7.108(13)</b>
CaNdBaCuO	7.45	0.2	7.130	7.170	7.180		7.160(22)	7.160(12)
	7.25	0.1	6.972	6.972	6.980	6.973	6.974(3)	6.975(0)
	7.25	0.2	6.961	6.960	6.960	6.960	6.960(0)	6.963(1)
	7.25	0.3	6.948	6.954	6.958	6.948	6.952(4)	6.941(2)

the above parameters the deviation between measured and calculated values of  $y_{M-I}^{av}$  does not exceed  $\sim 0.01$  (in most cases it is less than 0.005).

Having established a method to predict values of  $y_{M-I}$  of compositions  $Q$  and  $x$ , we proceed to examine whether it is possible to estimate other physical properties of materials that have not actually been prepared. Obviously, it would be possible to obtain  $T_c$  (with accuracy  $\sim \pm 2$  K in most of the range) from Fig. 5 if  $y - y_{M-I}$  is known, that is, for any given  $Q$ ,  $x$ , and  $y$ . Similarly, it is possible to obtain the room-temperature values of the TEP and resistivity. The plot of  $S_{290\text{K}}$  and  $\rho_{290\text{K}}$  vs  $y - y_{M-I}$  for the entire family is shown in Fig. 8. The curves are guides for the eye. Again we see that the various compositions coalesce into a single curve in each figure when the data are presented as function of  $y - y_{M-I}$ , although there is slight scatter ( $\sim \pm 0.01$ ) in  $y - y_{M-I}^{av}$  of the TEP data. There is also some scatter in the resistivity data probably due to granularity problems. From these ‘‘universal’’ curves, one could estimate  $S_{290\text{K}}$  of a specific sample with a given value of  $Q, x, y$  to within  $\sim \pm 2 \mu\text{V/K}$ . The accuracy in estimating  $\rho_{290\text{K}}$  is about  $\pm 50\%$ .

## V. DISCUSSION

### A. A single family of materials

The coalescence of our results when plotted against  $y - y_{M-I}(Q, x)$  (Figs. 5 and 8) suggests a one-to-one correspondence between this macroscopic parameter and the microscopic mobile hole (carrier) density in the  $\text{CuO}_2$  planes  $h$ . Therefore,  $y - y_{M-I}$  is the doping parameter in a large group of materials comprising various values of  $Q$ ,  $x$ , and  $R$ . We also provided indications (Fig. 5) that there exists a single  $T_c^{\text{max}}$  in these materials which therefore behave as a single family; that is, one can obtain physical properties as function of  $Q$ ,  $x$ , and  $y$  in a predictable manner. In order to make the existence of a single  $T_c^{\text{max}}$  more evident, we show in Fig. 9 our TEP results superimposed on the universal curve of  $S_{290\text{K}}$  (room-temperature TEP) vs  $T_c/T_c^{\text{max}}$  typical of many cuprates, which has been reproduced from Obertelli *et al.*<sup>1</sup>

Notice that samples having the same  $T_c$  also have the same TEP, irrespective of the values of  $x$ ,  $y$ ,  $Q$ , or  $R$  (Fig. 9). For instance, for  $R = \text{La}$  and  $Q = 7.25$  one observes for samples with  $T_c = 27 \pm 0.8$  or  $65 \pm 1$  K ( $T_c$  is not shown in the figure), that  $T_c/T_c^{\text{max}} \cong 0.33$  or  $0.80$  and that  $S_{290\text{K}} \cong 41$  or  $12 \mu\text{V/K}$ , respectively, *independent of  $x$  or  $y$* . Thus  $T_c^{\text{max}}$  is constant to within about  $\pm 3\%$ . Had there been different values of  $T_c^{\text{max}}$  for the various compositions, the results of samples with the same  $T_c$  would not coincide.

The measurements presented so far suggest that  $T_c^{\text{max}}$  and  $y - y_{M-I}$  are two independent parameters that determine  $T_c$ . This is supported by our recent pressure measurements on  $\text{CaLaBaCuO}$ .<sup>10</sup> In the phenomenological analysis that we developed,<sup>10</sup>  $dT_c/dP$  receives two independent contributions from the pressure dependence of  $T_c^{\text{max}}$  and  $y - y_{M-I}$ . Our analysis yields a linear dependence of the pressure derivative on the doping parameter, which was confirmed by our results over a wide range of doping.<sup>10</sup> This allows one to predict the variation of  $dT_c/dP$  with doping over the entire range of superconductivity. These observations also provide a clue to the microscopic origin of  $y - y_{M-I}$ . In the derivation of  $dT_c/dP$ , we assumed  $y_{\text{opt}} - y_{M-I}$  to be independent of pressure ( $y_{\text{opt}}$  is the value of  $y$  at optimal doping). Our results would not fit well the analysis without making this assumption. This suggests that  $y_{\text{opt}} - y_{M-I}$  (and more generally  $y - y_{M-I}$ ) is related to the number of states in the  $\text{CuO}_2$  band because the total number of states between the M-I transition and optimal doping is expected to be independent of pressure provided that the symmetry of the crystal is preserved. Moreover,  $y_{\text{opt}} - y_{M-I}$  is also independent of  $Q$  and  $x$ .<sup>9,10</sup> This can be seen directly by inspection of Fig. 5. For instance, in the present family  $y_{\text{opt}} - y_{M-I} \cong 0.29$ .<sup>10</sup> Thus, the number of states in the band appears to be constant independent of  $Q$  and  $x$ .

In the context of pressure measurements our results of lattice parameters are also worthy of mention. Samples with different compositions having similar values of  $dT_c/dP$ ,<sup>10</sup> also have the same  $T_c$  but rather different lattice parameters (Sec. III A). This suggests that the changes in  $T_c$  and the variation in lattice parameters that occur concurrently under

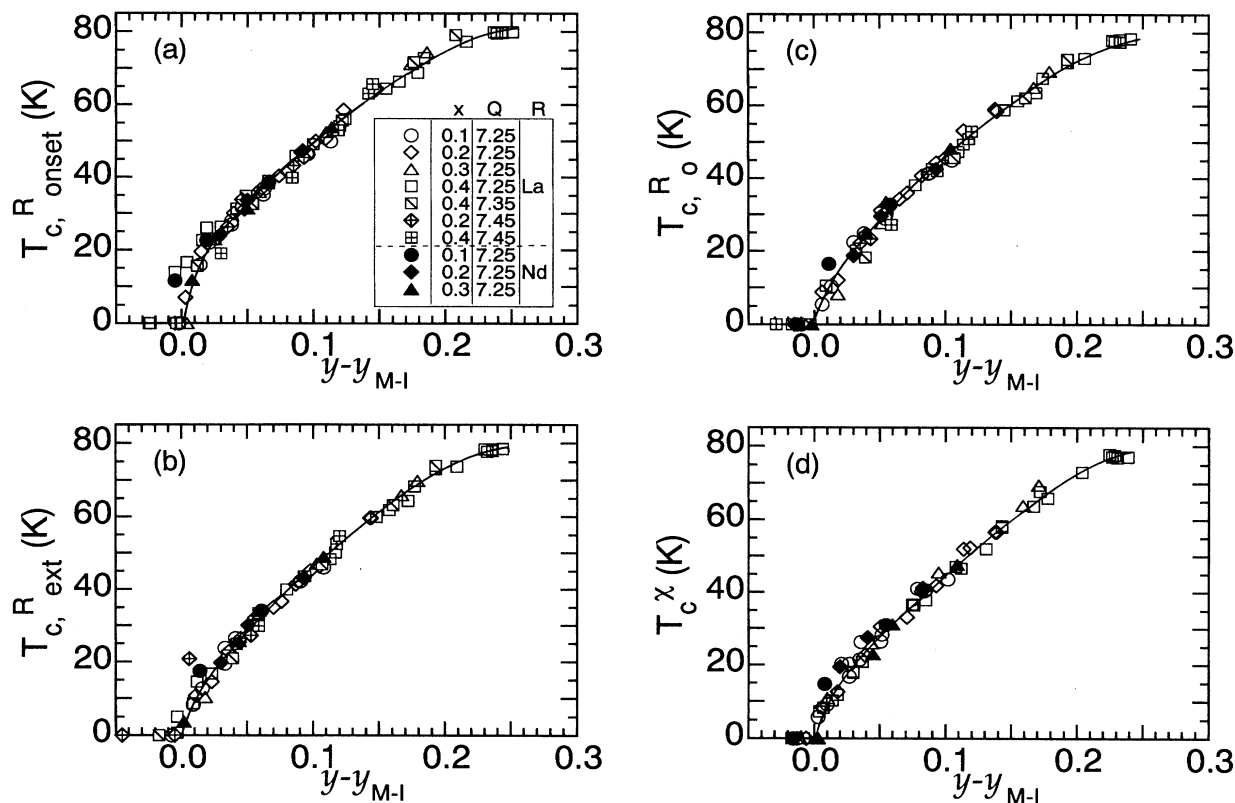


FIG. 5. Dependence of  $T_c$  on the doping parameter  $y - y_{M-I}$  ( $Q, x$ ) for the entire family of materials. For each definition of  $T_c$ , the measured value of  $y_{M-I}$  shown in Table I, was used.

pressure, are not directly related to one another. Perhaps the effect on interatomic distances due to the hydrostatic nature of the applied pressure is different from the effect due to atomic substitutions.

## B. Modified band picture

### 1. The simple band picture

Our results support some aspects of the band picture in cuprates, e.g., such as employed in the van Hove scenario.<sup>13</sup> In particular, a single band (the  $\text{CuO}_2$  band) is responsible for superconductivity and transport. (Notice that the materials are tetragonal, lacking chain order. Hence, the chain band is probably completely disordered and unlike in  $\text{YBaCuO}$ ,<sup>14,15</sup> is not expected to contribute to transport or to superconductivity.) In this simple single band picture, it is likely that  $y - y_{M-I}$  represents the integrated spectral density (i.e., the number of states) in the  $\text{CuO}_2$  band as was suggested above. It is related, through the shape of the density of states (DOS), to the energy difference between the top of the band and  $E_F$  [see Fig. 10(a)]. In materials where  $y_{M-I}$  (that is,  $Q$  and  $x$ ) is constant, such as well annealed  $\text{YBa}_2\text{Cu}_3\text{O}_{7-\delta}$  ( $Q=7$ ,  $x=0$ ),  $y - y_{M-I}$  is directly related to  $\delta$  in a simple way [i.e.,  $\Delta(y - y_{M-I}) = \Delta y = -\Delta\delta$ ] yielding the well-known dependence of physical properties on oxygen content. On the other hand the dependence of  $y_{M-I}$  on  $Q$  and  $x$  shows that

$y - y_{M-I}$ , and consequently the doping level, can change even when the oxygen content remains constant. The other independent parameter ( $T_c^{\text{max}}$ ) possibly represents in this picture the maximum in the DOS in this band (in the sense of the BCS formula). In that case the maximal DOS remains constant in the extended family despite chemical changes. Since the number of states also remains constant, the entire spectral shape of the DOS should not change much.

### 2. Modification of the band picture to account for isoelectronic doping

However, the band picture in Fig. 10(a) is not complete. Recall that we observed big changes in  $T_c$  and transport properties under isoelectronic conditions where the average electron (or hole) concentration remains constant.<sup>9</sup> [This can be seen directly by inspection of Fig. 3(b) where  $T_c$  varies at constant  $y$  while  $x$  changes. As  $Q$  remains constant in these samples, a constant  $y$  would mean that the average (chemical) hole concentration remains constant independent of  $x$ .] At the same time no new states are added near  $E_F$  since the oxygen content is kept constant (provided that addition of  $\text{Ca}^{2+}$  and removal of  $\text{Ba}^{2+}$  with increasing  $x$  does not in itself yield a significant increase in the number of states of these ions near  $E_F$ ). Therefore, the band picture presented in Fig. 10(a) is insufficient to explain our isoelectronic results. Additional states are required near  $E_F$  that get uncovered as

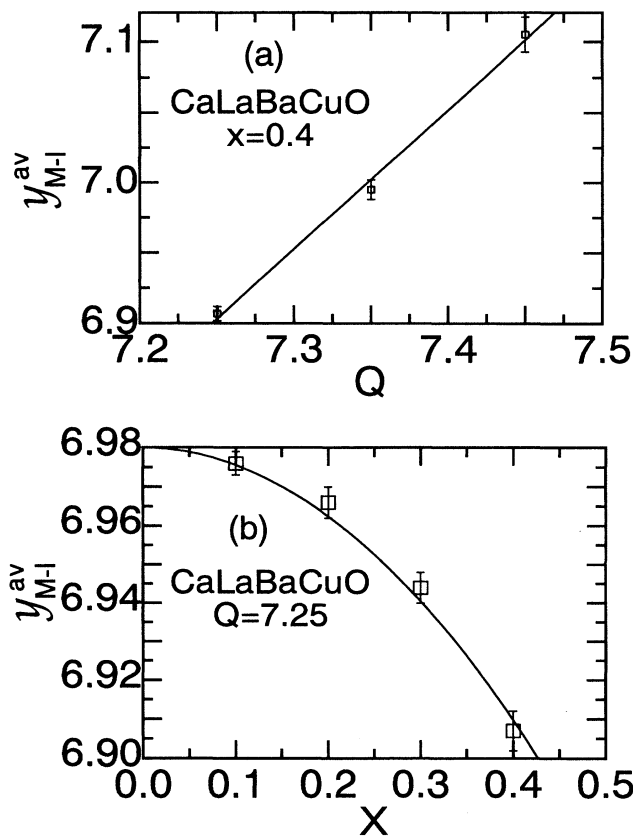


FIG. 6. Dependence of  $y_{M-I}^{av}$ , the measured average value of  $y_{M-I}$  (a) on the cation charge  $Q$ , and (b) on the composition  $x$ .

isoelectronic doping proceeds, thereby making room for electrons that were released from the  $\text{CuO}_2$  band. Hence, we postulate the existence of low-mobility states that do not contribute to superconductivity or transport, preserving the single-band nature of our results. Another indication that these states are of low mobility is the behavior below the M-I

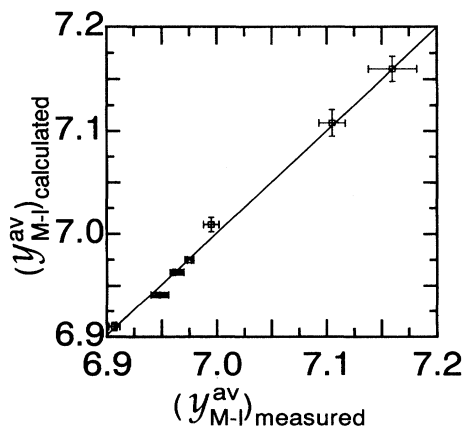


FIG. 7. The average value  $y_{M-I}^{av}$  calculated from the empirical formula [Eq. (1)], as compared with the measured value. The line is a least-squares fit of the data.

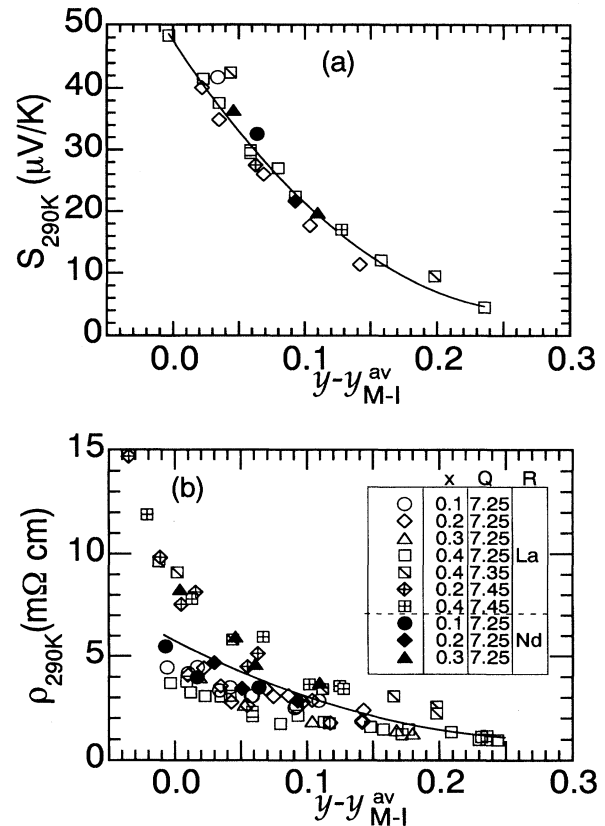


FIG. 8. Dependence of the room-temperature transport properties on the doping parameter  $y - y_{M-I}^{av}$  for the entire family: (a) thermoelectric power, (b) resistivity.

transition. Had these states been of high-mobility nature, one would expect a metallic rather than a semiconductorlike behavior that is observed near and below the M-I transition.<sup>7,9</sup> These low-mobility states should be degenerate in energy with the  $\text{CuO}_2$  band [see Fig. 10(b)]. Otherwise they cannot affect the chemical potential; in other words, they would be either fully occupied or empty and their occupation would not change with substitution. Moreover, since no new states are added, this requires a *relative band shift* of the mobile states (MB) with respect to the low-mobility states (LB). As shown in Fig. 10(b), with increasing  $x$  (at constant  $Q$ ) the  $\text{CuO}_2$  band moves upward relative to the low-mobility states. In this sense our picture differs from the regular band picture.

The existence of a MB and a LB and their relative shift upon isoelectronic doping makes it more difficult to provide a microscopic interpretation for  $y - y_{M-I}$ . For instance, it is not clear whether this parameter is related to the DOS of both bands or only to that of the MB. It is plausible to assume that the LB is involved in the determination of  $y - y_{M-I}$  since it affects the chemical potential. However, as in the simple band picture, there still should be a one to one correspondence between  $y - y_{M-I}$  and  $h$ , the number of mobile holes in the MB alone. Thus,  $y - y_{M-I}$  is still related to the energy difference between the top of the MB and  $E_F$ .

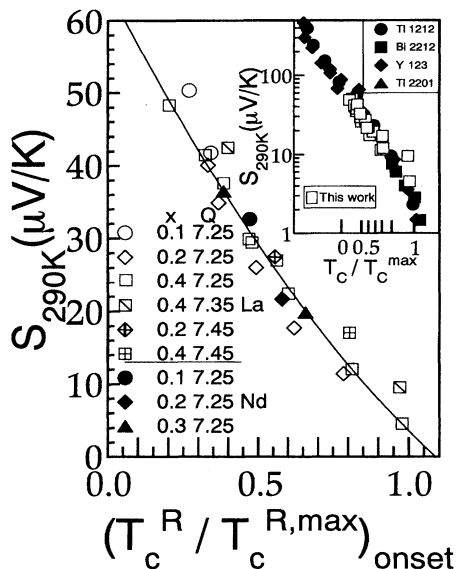


FIG. 9. Dependence of the room-temperature thermoelectric power on  $T_c/T_c^{\max}$ . Coalescence into a single curve of the results for samples having the same  $T_c$  yields a single  $T_c^{\max}$  for the entire family (see text). Inset: same data (open symbols) superimposed on the universal thermoelectric power plot of Obertelli *et al.* (dark symbols). See Ref. 1.

This could happen if, besides the MB, the spectral shape of the DOS of the LB remains unchanged among these materials and is besides a slowly varying function of energy. In Fig. 10(b), a constant DOS was used as a representative of the LB. We would like to emphasize again that within this modified band picture the relative band shift is an important conclusion. The only way for the system to adjust itself so as to change the density of mobile holes, keeping at the same time the total hole concentration constant, is by means of these relative band shifts. In principle, such behavior could result also from carrier localization due to disorder, e.g., cation disorder that might exist in the vicinity of the (Ca,La) and (La,Ba) planes. In that case the disorder is expected to increase (and hence  $h$  to decrease) when  $x$  and perhaps also  $Q$  increase. However,  $T_c$  and transport improve with increasing  $x$ . Besides, the parameter that determines  $T_c$  and transport ( $y - y_{M-I}$ ) reflects the doping behavior, not cation disorder. Moreover, localization — as might be indicated by the semiconductorlike behavior of  $\rho(T)$  — occurs only close to the M-I boundary.<sup>9</sup> At higher  $y$  there is no sign of localization. Therefore we think it unlikely that disorder-induced localization explains our isoelectronic doping results.

### 3. Implications of the modified band picture

Probably, similar band shifts accompany also regular doping conditions, e.g., when the oxygen content or cation charge are changed. In this case, however, such band shifts are not easily discernible due to addition of states with increasing  $y$  and due to our inability to separate contributions to the microscopic hole density from various sources. These band shifts complicate the relation between  $h$  and the chemi-

cal hole concentration  $n$ . In fact, in Fig. 11 we show that various relationships are possible depending on the doping conditions. For instance, it is possible for  $n$  to remain constant while  $h$  increases (path 1). It is also possible for  $n$  to increase while  $h$  remains constant (path 2) since  $y$  increases but  $T_c$  is constant, or that  $n$  and  $h$  decrease simultaneously (path 3). In other words, there does not seem to exist a simple relationship between  $h$  and  $n$ . The straightforward relationship that does exist in these materials is between  $h$  and  $y - y_{M-I}$ . The latter might be considered as a “relative chemical charge,” but it cannot be obtained from first principles since  $y_{M-I}$  cannot be calculated from simple chemistry. As long as a theory for calculating  $y_{M-I}$  is not available, one could use the empirical approach [Eq. (1)] that was developed in this work.

Another implication of the relative band shift concerns the number of holes contributed when only Ca is substituted for Y (or only La for Ba) in YBaCuO. Due to hole splitting between the MB and LB and due to the relative band shifts this number is not necessarily equal to one per substituted atom, as was assumed in Ref. 2. (See Introduction.) Instead, hole splitting occurs as denoted by the arrows in Fig. 10(b), and at the same time the bands may shift. [The relevant levels of the Ca and La ions are also shown. The reason for placing the energy levels as shown is that the La ion donates the extra electron (relative to the regular charge of +2 on the Ba site) from its  $5d^1$  energy level which lies much above the  $\text{CuO}_2$  band. Similarly, the Ca ion receives the extra electron to its core level.] Moreover, since the degree of hole splitting may change with doping (for instance, as the DOS of the MB varies with energy) the number of mobile holes that actually go to the  $\text{CuO}_2$  band at each energy may change as function of doping. Generally speaking, one can only say that at a given doping level each substituted atom contributes the same fraction of a mobile hole or electron in proportion to the amount substituted. For this reason, we believe, there exist  $T_c$  and transport results which correspond to an increase in  $h$  that is smaller than one per substituted atom.<sup>16</sup> Notwithstanding, this number could become close to one if the hole splitting between the LB and MB is eventually compensated by the relative band shift which generates more holes. We would like to note though, that it is unlikely that our modified band model explains the symmetry observed in Ref. 2 upon separate Ca and La substitutions (see Introduction). Band shifts are likely to exist also when each atom is substituted separately. In fact, our cosubstitution results on charge-compensated materials suggest that such a symmetry does not exist and that the addition of Ca shifts the material more towards optimal doping.

It should also be noted that the existence of the LB helps explain the behavior of the TEP in the vicinity of the M-I transition. The value of the TEP near  $y_{M-I}$  ( $\sim 50 \mu\text{V/K}$ ) is not large; compared with other oxide semiconductors it is about an order of magnitude smaller at more or less the same hole or electron concentration.<sup>17</sup> Large values as in semiconductors would be expected once the MB becomes full provided that it is the only band in the vicinity of  $E_F$ . However, since the LB is degenerate with the top of the MB, electron excitation from the MB to the LB is possible at any finite temperature leaving behind mobile holes. These then account for

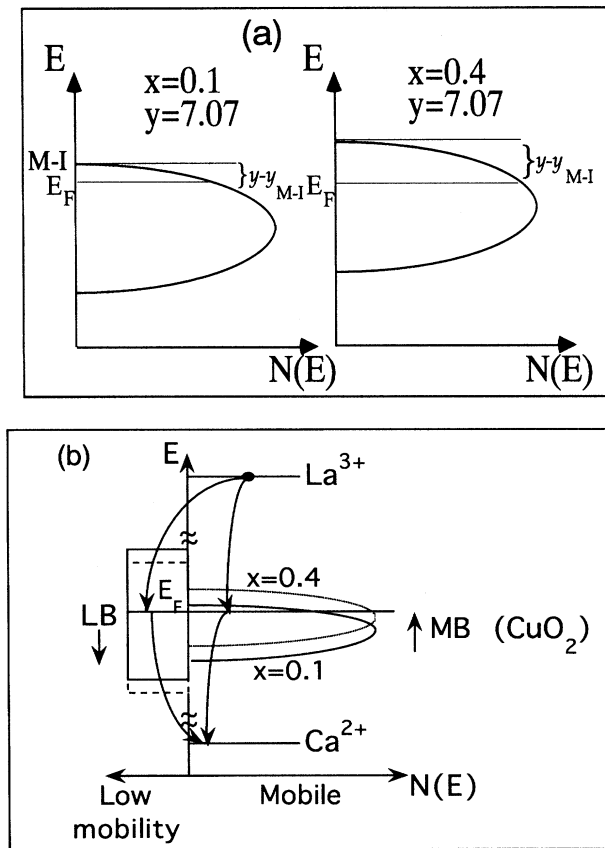


FIG. 10. Schematic presentation of the band picture. (a) Single-band picture, describing the change in energetics of the  $\text{CuO}_2$  band that presumably occur upon isoelectronic doping. In this scheme, electrons released from the mobile band do not have empty states where they could go. (b) Modified band picture. Low-mobility (LB) states have been added in degeneracy with the mobile band (MB). Isoelectronic doping at constant hole concentration occurs when electrons released from the MB are captured, via a relative shift of both bands, in states within the LB that get uncovered, thereby preserving the total number of electrons. For clarity, we used the Fermi energy of each composition  $x$  as the reference energy at that composition. Also notice that electrons donated by La substitution or holes generated by Ca substitution are split between the MB and LB. The degree of splitting may vary with doping depending on the spectral shape of both bands.

the relatively low TEP. A different point of view of the TEP problem near the M-I transition has been proposed by Oberthelli et al.<sup>1</sup> They suggest that the TEP is *large* compared to that in regular metals. In the unmodified band picture which was used in that work, these authors invoke a mobility edge *inside* the MB when  $y = y_{M-I}$ .

Within our modified band picture, the origin of the LB deserves further study. It might be interesting to perform calculations of band structure in this family (at constant  $Q$ ) in order to examine the evolution of bands with the amount of Ca substitution. Such calculations might be helpful in locating the origin of the LB among the various layers that exist in the unit cell (e.g., the basal plane or other parts of the

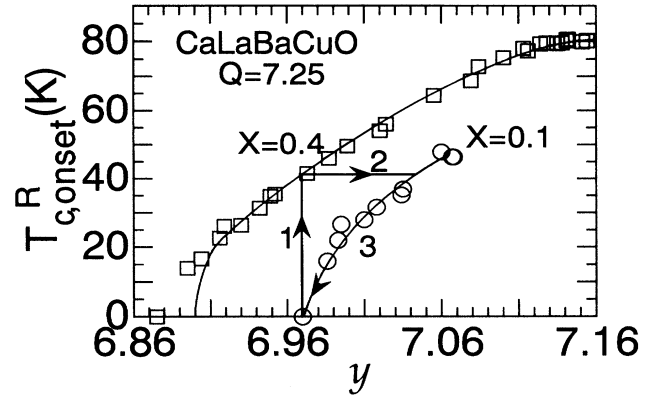


FIG. 11. Dependence of  $T_c$  on oxygen content showing that the relation between microscopic hole density  $h$  and chemical hole concentration  $n$  is not straightforward. First,  $n$  can remain constant while  $h$  increases (path 1, isoelectronic conditions). Second,  $n$  can increase while  $h$  is constant (path 2, iso  $T_c$  or iso TEP conditions). Finally,  $n$  can decrease while  $h$  decreases to its initial value (path 3, isocompositional conditions).

unit cell). Of particular interest would be an examination of the origin of the relative band shifts.

### C. Doping within the strong correlations picture

It is plausible to assume that the condition  $y = y_{M-I}$  corresponds to a full band. However, in  $\text{YBaCuO}$ ,  $y_{M-I}$  occurs roughly at 6.5, i.e., when Cu is in the +2 valence state. Electron counting based on simple band calculation arguments shows that  $\text{YBa}_2\text{Cu}_3\text{O}_{6.5}$  should be a metal because at this oxygen stoichiometry the  $\text{Cu}^{2+}$  ion has the odd electron  $3d^9$  configuration, and the  $3d_{x^2-y^2}$  orbital becomes half filled.<sup>18</sup> It would therefore be tempting to try to explain our doping results within the strong electron correlation picture. In this picture, the half-filled band splits into two subbands due to strong on site Coulomb repulsion between electrons of opposite spins, and a gap (the Hubbard gap) opens up. Thus, at half filling the lower subband is filled while the upper subband remains empty yielding the observed insulator behavior.<sup>18</sup> Recently, a doping theory within the correlation picture has been proposed by Unger and Fulde.<sup>19</sup> In this theory states are transferred from the upper Hubbard band to the vicinity of  $E_F$  when the microscopic hole density in the  $\text{CuO}_2$  planes is increased relative to half filling (hf). In principle, these additional states could provide the missing states required to capture the released electrons when the composition  $x$  is changed. However, in isoelectronic doping the chemical hole concentration remains constant and it is not clear *a priori* whether the hole density in the planes should actually change. If it does, we suspect that this again requires a shift of states associated with the planes relative to states associated with the rest of the crystal. This brings us back to the modified band picture. There also seems to exist a difficulty with identifying the M-I transition with half filling. When all three copper ions are in the oxidation state +2, one

can estimate  $y_{\text{hf}}$ , the oxygen concentration at half filling, from  $y_{\text{hf}} = \frac{1}{2}(Q + 3 \cdot 2) = 6.625$  for  $Q = 7.25$ . However, we have seen (Table I) that  $y_{\text{M-I}}$  lies between  $\sim 6.9$  and  $\sim 7.0$  for various values of  $x$ . The M-I transition seems to occur at hole concentrations *much higher* than half filling. This by itself may require that additional states exist in the vicinity of the plane states (due to the large number of states between half filling and M-I boundary, these are probably intrinsic states of the crystal, i.e., states that are not associated with impurities), in accordance with the modified band picture. Moreover, from the chemical count  $dy_{\text{hf}}/dQ = \frac{1}{2}$  whereas in the empirical equation [Eq. (1)] we saw that  $dy_{\text{M-I}}/dQ = \alpha \approx 1$  perhaps suggesting that  $y_{\text{M-I}}$  is not related with half filling of the parent band.

Another theory that includes the effect of correlations on the bands of excited states, has been proposed very recently by Dagotto *et al.*<sup>20</sup> They have shown that, when holes are treated as quasiparticles strongly dressed by the surrounding AF spin fluctuations, they yield the van Hove singularity as well as the superconductor pairing. This theory yields as a natural consequence the AF insulator phase as well as  $d$ -type symmetry of the superconducting order parameter and, at the same time, is also capable of explaining the existence of optimal doping. We would like to point out that, since doping effects are still associated with DOS considerations, we believe that the existence of additional states (LB) is also required within this theory in order to explain isoelectronic doping.

Still another strong correlation theory that is based on the polarizability or screening of the oxide background has been proposed recently by Weger *et al.*<sup>21</sup> Variation of physical properties, that according to other theories results from change in the hole density, arises in this theory mainly from oxide polarizability that could change with chemical substitution. In this sense one should consider a polarizability reservoir rather than a charge reservoir.<sup>22</sup> The microscopic parameter that determines the shape of the DOS and the strength of the pairing interaction is the dielectric screening  $\epsilon_0/\epsilon_\infty$  which could change with composition  $x$ . In turn, these quantities determine transport properties and  $T_c$ . It is, however, too early to say whether this microscopic parameter can be related to  $y - y_{\text{M-I}}(x)$ . For an *ab initio* calculation of this parameter the dielectric function has to be known over a wide frequency range, which does not seem to be presently available.<sup>22</sup>

## V. SUMMARY

We have shown that  $(\text{Ca}_x\text{R}_{1-x})(\text{Ba}_{3-z-x}\text{R}_{z-(1-x)})\text{Cu}_3\text{O}_y$  exists as high-purity single phase in a wide range of compositions for both  $R = \text{La}$  and  $\text{Nd}$ . All materials except those with compositions close to  $x = 0$ ,  $Q = 7$  ( $z = 1$ ) have the tetragonal 1:2:3 structure, form easily, and allow a systematic investigation free of the plateau structure. Having a single  $T_c^{\text{max}}$  (Figs. 5 and 9), these materials all behave as a single family strongly suggesting that the MB of Fig. 10(b) controls superconductor (and transport) properties. Doping occurs as usual by changing the oxygen content  $y$  or the noncopper cation charge  $Q$  ( $Q = 6 + z$ ). Interestingly, doping is also obtained in this charge compensated family even when  $y$  and  $Q$  are held constant [Fig. 3(b), Fig. 11, path 1], that is, when the

average (chemical) hole concentration remains constant (isoelectronic conditions). This implies that additional charge transfer from planes to the charge reservoir occurs. Such doping must be accompanied by changes in band structure. Specifically, there should exist also low-mobility (LB) states in the vicinity of  $E_F$  that get uncovered as isoelectronic doping proceeds. Doping, i.e., transfer of electrons from the MB to the LB, can occur only if there is a *relative band shift* of the MB with respect to the LB [Fig. 10(b)]. Our modified band picture differs from the conventional band picture in the existence of a LB degenerate with the MB and, in particular, the relative shift of both bands.

We have shown that for all compositions there exists a single macroscopic parameter  $y - y_{\text{M-I}}(Q, x)$ , the “relative chemical charge,” that determines the doping level. This is demonstrated in the behaviour of  $T_c$  (Fig. 5) and of the TEP and resistivity (Fig. 8) where the curves of these quantities each coalesce into a single curve when plotted as function of  $y - y_{\text{M-I}}$ . This doping parameter is related to the number of states in both the MB and LB. Nevertheless, there should still be a one to one correspondence between  $y - y_{\text{M-I}}$  and  $h$  the hole density in the MB only, suggesting that the DOS of both bands remains essentially unchanged among these materials.  $y_{\text{M-I}}$ , that varies as function of  $Q$  and  $x$  but seems to be independent of  $R$  for  $R = \text{La}$ , and  $\text{Nd}$ , cannot be obtained from simple chemical arguments. Lacking a theoretical approach to calculate  $y_{\text{M-I}}$ , we developed an empirical procedure of estimating  $y_{\text{M-I}}$  as function of  $Q$  and  $x$  [Eq. (1)]. This can be used to predict  $y_{\text{M-I}}$  in tetragonal 1:2:3 materials (i.e.,  $\text{CaR}\text{BaCuO}$  and probably also others), thereby allowing an estimate of physical properties such as  $T_c$ ,  $\rho$ , and TEP of these materials without actually preparing them. (One would use for this purpose the average values obtained from Figs. 5 and 8.)

It should be noted that separate substitution of one Ca or one La atom does not usually introduce or extract one mobile hole to the system [Fig. 10(b)]. Instead, the hole or electron would split between the MB and LB according to the DOS of both bands at  $E_F$ . When both Ca and La are cosubstituted in equal amounts, doping occurs despite total charge compensation due to charge redistribution that takes place when the bands shift one with respect to the other. The relative band shift complicates the relationship between microscopic hole density  $h$  and chemical hole concentration  $n$ . There does not seem to exist a straightforward relationship between both quantities (Fig. 11). On the other hand, our work suggests a close relationship between  $h$  and  $y - y_{\text{M-I}}$ .

We believe that the existence of a single macroscopic doping parameter  $y - y_{\text{M-I}}$  is of general significance in cuprates. It shows that effects on doping due to cation substitution or change in oxygen content can be casted into a single parameter. This result was unexpected since changes in  $y$  involve states that lie relatively close to  $E_F$  while changes in  $Q$  due to substitution of Ca (or La) involve states that mostly lie further away from the  $\text{CuO}_2$  band [Fig. 10(b)]. Presumably, cation substitution, besides adding or extracting an electron, also induces the relative band shifts thereby yielding the variation of  $y_{\text{M-I}}$  among materials as well as isoelectronic doping. It might not be easy to explain our results within the strong correlation doping theories without explicitly assuming the existence of additional states

besides the plane states and, more importantly, the existence of relative shifts of these states that occur upon substitution. This brings us back to the modified band picture.

#### ACKNOWLEDGMENTS

We would like to thank A. -K. Klehe and J. S. Schilling for their agreement to mention the pressure results prior to

publication. This research was supported by The Israel Science Foundation administrated by The Israel Academy of Sciences and Humanities, and by the Technion V.P.R. Fund—Posnansky Fund in High Temperature Superconductivity. The research was also supported by the Center for Absorption in Science, Ministry of Immigrant Absorption, State of Israel.

- 
- <sup>1</sup>S.D. Obertelli, J.R. Cooper, and J.L. Tallon, *Phys. Rev. B* **46**, 14 928 (1992).
- <sup>2</sup>J.J. Neumeier and H.A. Zimmermann, *Phys. Rev. B* **47**, 8385 (1993).
- <sup>3</sup>Y. Tokura, J.B. Torrance, T.C. Huang, and A.I. Nazzal, *Phys. Rev. B* **38**, 7156 (1988).
- <sup>4</sup>D. Goldschmidt, G.M. Reisner, Y. Direktovitch, A. Knizhnik, E. Gartstein, G. Kimmel, and Y. Eckstein, *Physica C* **217**, 217 (1993).
- <sup>5</sup>D. Goldschmidt, Y. Direktovitch, A. Knizhnik, and Y. Eckstein, *Phys. Rev. Lett.* **71**, 3392 (1993).
- <sup>6</sup>D. Goldschmidt, A. Knizhnik, Y. Direktovitch, G.M. Reisner, and Y. Eckstein, *Phys. Rev. B* **49**, 15 928 (1994).
- <sup>7</sup>D. Goldschmidt, G.M. Reisner, Y. Direktovitch, A. Knizhnik, E. Gartstein, G. Kimmel, and Y. Eckstein, *Phys. Rev. B* **48**, 532 (1993).
- <sup>8</sup>A. Knizhnik, Y. Direktovitch, D. Goldschmidt, and Y. Eckstein, *Supercond. Sci. Technol.* **6**, 209 (1993).
- <sup>9</sup>D. Goldschmidt, Y. Direktovitch, A. Knizhnik, and Y. Eckstein, *Phys. Rev. B* **51**, 6739 (1995).
- <sup>10</sup>D. Goldschmidt, A.-K. Klehe, J.S. Schilling, and Y. Eckstein (unpublished).
- <sup>11</sup>J.S. Schilling and S. Klotz, in *Physical Properties of High Temperature Superconductors*, edited by D.M. Ginsberg (World Scientific, Singapore, 1992), Vol. III, p. 59.
- <sup>12</sup>J.M.S. Skakle and A.R. West, *Physica C* **220**, 187 (1994).
- <sup>13</sup>C.C. Tsuei, *Physica A* **168**, 238 (1990); D.M. Newns, C.C. Tsuei, P.C. Pattnaik, and C.L. Kane, *Comments Condens. Matter Phys.* **15**, 273 (1992).
- <sup>14</sup>D. Goldschmidt and Y. Eckstein, *Physica C* **200**, 99 (1992).
- <sup>15</sup>R. Gagnon, C. Lupien, and L. Taillefer, *Phys. Rev. B* **50**, 3458 (1994).
- <sup>16</sup>B. Fisher, J. Genossar, C.G. Kuper, L. Patlagan, G.M. Reisner, and A. Knizhnik, *Phys. Rev. B* **47**, 6054 (1993).
- <sup>17</sup>G.M. Choi, H.L. Tuller, and D.G. Goldschmidt, *Phys. Rev. B* **34**, 6972 (1986); D. Goldschmidt and H.L. Tuller, *ibid.* **34**, 5558 (1986).
- <sup>18</sup>See, for instance, in *Transition Metal Oxides*, edited by P.A. Cox (Clarendon Press, Oxford, 1992), Sec. 5.4.
- <sup>19</sup>P. Unger and P. Fulde, *Phys. Rev. B* **48**, 16 607 (1993).
- <sup>20</sup>E. Dagotto, A. Nazarenko, and A. Moreo, *Phys. Rev. Lett.* **74**, 310 (1995).
- <sup>21</sup>M. Weger and D. Wohlleben, *Z. Phys. B* **87**, 143 (1992); M. Weger, *Low Temp. Phys.* **95**, 131 (1994).
- <sup>22</sup>M. Weger (private communication).